Multiscale Turbulence Effects in Underexpanded Supersonic Jets

Khaled S. Abdol-Hamid*
Analytical Services and Materials, Inc., Hampton, Virginia
and
Richard G. Wilmoth†
NASA Langley Research Center, Hampton, Virginia

A modified version of the multiscale turbulence model of Hanjalic has been applied to the problem of underexpanded supersonic jets. In particular, the shock-cell decay resulting from shock-mixing layer interactions has been studied for both mildly interacting and strongly resonant jet conditions. A verision of the Hanjalic et al. model, which accounts for nonequilibrium energy transfer between two spectral scales of turbulence, was incorporated into an existing shock-capturing, parabolized Navier-Stokes computational model in order to perform numerical experiments. Results are presented for nominal initial jet Mach numbers of 2.0, 1.4, and 1.0 and are compared to experiments and to predictions made using single-scale models. The results show significant effects of multispectral turbulent energy transfer on the predicted shock-cell decay, particularly for the lower jet Mach numbers.

Nomenclature

$C_\mu, C_{P1}, C_{P2}, C_{T1}, C_{T2}$ = turbulence model coefficients
h = static enthalpy
H = total enthalpy ($= h + \frac{1}{2}Q^2$)
k_P = production turbulence energy
k_T = transfer turbulence energy
M = Mach number
M_e = fully expanded jet Mach number
M_j = nozzle-exit design Mach number
P = static pressure
$\underline{P}$ = production rate of turbulent kinetic energy
P_a = ambient static pressure in still air
P_j = static pressure in jet at nozzle exit
Q = total velocity
r = transverse distance
r_L, r_U = lower and upper mixing layer boundaries
U = streamwise mean velocity
u, v = instantaneous velocity fluctuations
V = transverse mean velocity
$\bar{v}\bar{\gamma}$ = time-averaged components of Reynolds stress and/or turbulent heat or concentration fluxes
W = turbulent vorticity
x = streamwise distance
γ = $\gamma = u, v, h,$ or ϕ
ϵ_p = dissipation rate of production turbulent kinetic energy
ϵ_T = dissipation rate of transfer turbulent kinetic energy
μ = molecular viscosity
μ_{eff} = effective viscosity ($= \mu + \mu_t$)
Φ = species mass fraction parameter
ρ = gas mixture density
σ_f = effective Prandtl number

Received Aug. 4, 1987; revision received April 7, 1988.

*Research Scientist. Member AIAA.
†Aerospace Engineer, Propulsion Aerodynamics Branch, Transonic Aerodynamic Division.

Introduction

OVER the last several years, significant progress has been made toward developing both an understanding of and a predictive capability for the dominant physical processes in turbulent supersonic jets. Advances in computational fluid dynamics have produced numerical models such as the SCIPVIS code of Dash and Wolf[1] that can predict quantitatively many of the details of the shock-cell structure, the turbulent mixing with an external stream, and the subsequent decay of the shock-cell strength due to shock/mixing-layer interactions. The fundamental understanding of such phenomena has been enhanced through the development of analytical models such as that of Tam, Jackson, and Seiner,[2] which is based on a linear solution for the shock-cell structure using the method of multiple-scale asymptotic expansions. Although the numerical models generally are more useful for quantitative predictions, particularly for nonlinear problems, the analytical wave models can more readily provide information on the spectral components of the flowfield. Both models have proven to be useful for predictions related to broadband shock noise[2-4] for mildly underexpanded and mildly overexpanded plumes. The SCIPVIS code also can give accurate predictions of the near-field plume shock structure for highly underexpanded and highly overexpanded cases so long as the flowfield is mainly dominated by inviscid processes.

However, it has been observed[2,3] that in situations where strong interactions between the shock structure and large-scale turbulent structure are suspected to occur, neither model adequately predicts the shock-cell decay. In such situations, the relative wavelengths of the turbulent and inviscid structures are such that acoustically stimulated production of large-scale

structures is believed to occur, and the plume decays or collapses rapidly after a few shock cells. The turbulent processes are in some sense similar to the breakup frequently observed in low-speed jets and shear layers due to the instability of the flow. In each case, a mechanism for the transfer of energy between different scales of turbulence is required to explain the phenomena.

The numerical model of Dash and Wolf[1] and the analytical model of Tam et al.[2] use turbulence models to describe the mixing between the jet and the surrounding stream that are based on the assumption of a spectral distribution of turbulent eddies that remains in equilibrium. For the equilibrium assumption to hold, the time scales for the transfer of energy between different turbulence scales must be much different from the time scales associated with the overall production and dissipation of turbulence. In such caes, only a single spectral scale need be considered, since the spectral distribution does not change over the time scale of interest. However, when these time scales are not greatly different, it would appear that some modeling of multiscale turbulence effects is needed.

Hanjalic et al.[5] have proposed a turbulence closure scheme employing two or more independently calculated time scales to describe the rates of different turbulent interactions. The model was tested with relatively good success for several classes of boundary-layer, free-shear, and jet-mixing problems. Chen[6,7] adapted the model to the problems of confined swirling jet and recirculating flows with good results. The Hanjalic model adapted by Chen follows the gradient transport formulations of Launder et al.,[8,9] with the addition of new equations to describe the transfer of energy between the two scales. Wilcox[10] has proposed a two-scale closure model that decomposes the Reynolds-stress tensor into "large" and "small" eddies and has applied the model with good success to several boundary-layer and shear-flow problems. Each of these models appears to have some merit for studying problems where a multiscale spectrum of turbulence is expected to be important. However, the Hanjalic model adapted by Chen appears to be somewhat simpler to implement in numerical jet models such as the SCIPVIS code.

In the present paper, the multiscale turbulence model of Hanjalic is applied to the problem of underexpanded supersonic jets. In particular, the shock-cell decay resulting from shock-mixing layer interactions is addressed for both mildly interacting and strongly resonant jet conditions. A typical flowfield for an underexpanded shock-containing, supersonic jet plume is shown in Fig. 1. The Hanjalic model was incorporated into the SCIPVIS code in order to perform numerical experiments. The approach was to formulate a two-scale set of parabolized turbulent-energy and dissipation-rate transport equations that essentially were identical to the one-scale, two-equation model of Launder et al.,[8,9] which was already contained within the SCIPVIS code. This required the addition of two new transport equations to describe the transfer of energy between scales. This approach is similar to that of Chen but is applied here to the steady, parabolic flow equations. The computational model then was applied to several experimental test cases of Seiner et al.[3] This paper summarizes the results of Abdol-Hamid and Wilmoth[11] and presents additional comparisons with experiment. Complete details of the turbulence model are given in Ref. 5.

Turbulence Models

Most of the numerical models that have been applied to predict the flow and heat transfer in jet-mixing problems are of the finite-difference type. These solve the time-averaged partial differential equations governing the turbulent transport of heat, mass, or species concentration using a finite-difference numerical approach. The equations describing the mean flowfield quantities for turbulent free shear are well known, e.g., see Tennekes and Lumley.[12] The mean flow equations for steady-state, two-dimensional flows may be expressed as

$$\frac{\partial \rho U r^J}{\partial x}+\frac{\partial \rho V r^J}{\partial r}=0 \tag{1}$$

for continuity and

$$\frac{\partial \rho U \Gamma r^J}{\partial x}+\frac{\partial \rho V \Gamma r^J}{\partial r}=\frac{\partial}{\partial r} r^J\left(\frac{\mu}{\beta_\Gamma}\frac{\partial \Gamma}{\partial r}-\rho\overline{v\gamma}\right)+S_\Gamma \tag{2}$$

for momentum or energy conservation, where Γ may stand for any of the velocity components (U and V), β_Γ is the thermal coefficient, and S_Γ is the corresponding source term given by

$$S_U=-r^J\frac{\partial P}{\partial x} \tag{3a}$$

$$S_V=-r^J\frac{\partial P}{\partial r} \tag{3b}$$

$$S_H=S_\Phi=0 \tag{3c}$$

In the above equations $J=1$ for axisymmetric flows, and $J=0$ for planar flows.

The derivation of Eq. (2) is based on the assumption that terms involving density and pressure fluctuations can be neglected compared to the turbulent transport terms. This follows Morkovin's hypothesis that ρ' has a small effect on turbulence structure if $\rho'/\rho \ll 1$. This allows the use of an incompressible turbulence model in a compressible flow for $M<5$ in a boundary layer and for $M<1$ in a mixing layer.[13,14]

To close Eqs. (1) and (2), additional equations must be prescribed to model the turbulence terms, and this is the main purpose of most turbulence models. Most turbulence closure schemes for shear flows follow Boussinesq's eddy-viscosity concept, which assumes that turbulent stresses and heat and concentration fluxes are proportional to the normal gradient in Γ. Thus, the diffusion terms $v\gamma$ may be expressed as

$$-\rho\overline{uv}=\mu_t\frac{\partial U}{\partial r} \tag{4a}$$

$$-\rho\overline{v^2}=2\mu_t\frac{\partial V}{\partial r}-\frac{2}{3}\rho k \tag{4b}$$

$$-\rho\overline{vh}=\frac{\mu_t}{\sigma_H}\frac{\partial H}{\partial r} \tag{4c}$$

$$-\rho\overline{v\Phi}=\frac{\mu_t}{\sigma_\Phi}\frac{\partial \Phi}{\partial r} \tag{4d}$$

In general, for $\gamma \neq v$, $-\overline{v\gamma}=(\mu_t/\beta_\Gamma)(\partial\Gamma/\partial r)$.

In Eqs. (4), μ_t is the turbulent eddy viscosity, which is not a fluid property but depends on the state of turbulence, and its value varies from point to point in the flowfield.

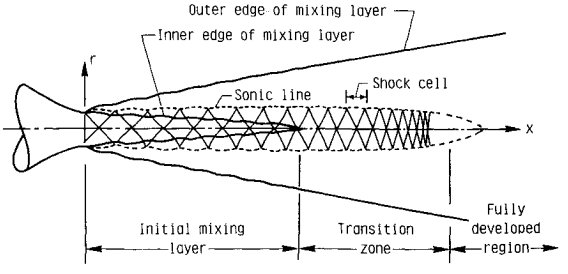

Fig. 1 Typical flowfield for underexpanded supersonic jet plume.

One-Scale Model

The additional closure assumption required is a model for μ_t. One of the most widely used models for the distribution of μ_t is the $k\epsilon$ (two-equation) turbulence model. According to this model

$$\mu_t = C_\mu \frac{\rho k^2}{\epsilon} \tag{5}$$

where k represents the velocity scale for the large-scale turbulent motion, ϵ is the rate of dissipation of the turbulent kinetic energy, and C_μ is a function to be prescribed. The distributions of k and ϵ are obtained from the solution of partial differential equations, which have the same form as Eq. (2), with

$$S_k = \underline{P} - \rho\epsilon \tag{6a}$$

$$S_\epsilon = (C_{P1}\underline{P} - C_{P2}\epsilon)(\epsilon/k) \tag{6b}$$

and the turbulent diffusion fluxes are obtained from Eqs. (4) by substituting k or ϵ for H. $\underline{P}$ is the rate of generation of turbulent kinetic energy (production) by the interaction of turbulent stresses with mean velocity gradients and is given by

$$\underline{P} = -\overline{uv}\frac{\partial U}{\partial r} \tag{7}$$

This model is based on the assumption that the flows considered are fairly close to a spectral equilibrium. Here, only one time scale k/ϵ is considered, and the times associated with the transfer of energy between different spectral regions are assumed to be negligible.

In the present paper, the more elaborate $k\epsilon 2$ turbulence model of Rodi,[15] including the compressibility corrected turbulence viscosity of Dash et al.,[16] is used. Abdol-Hamid and Wilmoth[11] provide a list of constants and coefficients and a brief discription of the correction functions.

In the rest of this paper, the $k\epsilon 2$ turbulence model with the compressibility correction function is referred to as *kε2-cc*.

Two-Scale Model

The basis of the approach used to model multispectral turbulence scales is described in detail by Hanjalic et al.[5] and Chen.[6,7] This two-scale model takes into account the nonequilibrium spectral energy transfer mechanism. The key to the two-scale model is the recognition that, whereas the one-scale dissipation and kinetic energy equations contain both production and dissipation terms, these processes occur in different spectral regions. The turbulent energy production occurs in the large eddies in the flow, whereas dissipation phenomena involve primarily the smaller scales.

Essentially, the kinetic energy is divided into roughly three regions: lage-scale energy production, intermediate energy transfer, and small-scale dissipation. At high Reynolds numbers, the energy content of the dissipative eddies is negligible. Thus, the turbulent kinetic energy may be divided into two parts: the large scale k_P (containing low wave number eddies), and high wave number transfer eddies k_T. Energy leaves the low wave number region at a rate of ϵ_T and enters the high wave number region at a rate ϵ_T. To simplify the modeling procedure, it has been assumed that spectral equilibrium exists between the transfer region and the dissipation region ($\epsilon = \epsilon_T$). This assumption results from considering only a single-transfer mechanism between two spectral scales. If more than one production scale and/or multiple-transfer regions are considered, the overall dissipation ϵ would not be in equilibrium with a single-transfer region.

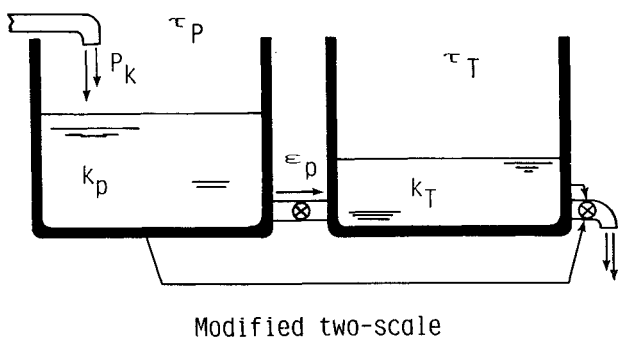

Fig. 2 Tank-and-tube analogy for spectral transfer of turbulent energy (from Hanjalic et al.[5]).

The basis of the two-scale model may be visualized through the use of the tank-and-tube analogy shown in Fig. 2. The amount of energy involved in transfer processes (shown as a tank of level k_T) is controlled by the difference in dissipation, $\epsilon_P - \epsilon_T$. Production of turbulence P feeds the kinetic energy tank designated by k_P; k_P and k_T represent the level of energy in each tank (production and transfer), whereas ϵ_P and ϵ_T are the valve restrictions of the corresponding tanks. Therefore, the time constants associated with filling the production and transfer tanks can be written in the following forms:

$$\tau_p = k_P/\epsilon_P \tag{8a}$$

$$\tau_T = k_T/\epsilon_T \tag{8b}$$

and the time-scale ratio is

$$T = \tau_T/\tau_P = (k_T/k_P)(\epsilon_P/\epsilon_T) \tag{9}$$

where T may be used to represent the relative rate of turbulent energy transfer between the large scale (production region) and intermediate scale (transfer region).

Following the one-scale model formulation described, the distribution of k_P, k_T, ϵ_P, and ϵ_T are obtained from the solution of partial differential equations that have the same form as Eq. (2) with

$$S_{k_P} = \underline{P} - \rho\epsilon_P \tag{10a}$$

$$S_{k_T} = \rho(\epsilon_p - \epsilon_T) \tag{10b}$$

$$S_{\epsilon_P} = (C_{P1}\underline{P} - C_{P2}\rho\epsilon_p)/\tau_p \tag{10c}$$

$$S_{\epsilon_T} = (\rho/\tau_P)(C_{T1}\epsilon_P - C_{T2}\epsilon_T) \tag{10d}$$

The values of the constants and coefficients used for the present calculations can be found in Ref. 11. Within the context of this paper, the two-scale version of $k\epsilon 2$ is referred to as *kε2-2S*, and the two-scale version of the compressibility corrected model is referred to as *kε2-2S-cc*.

Modified SCIPVIS Model

The *kε2-2S* and *kε2-2S-cc* turbulence models were incorporated into the SCIPVIS code to provide a computational framework for testing the importance of two-scale effects. The SCIPVIS code solves the steady-state, parabolized Navier-Stokes equations (streamwise diffusion terms neglected) by an explicit predictor-corrector spatial marching scheme. The pressure in the subsonic region of the mixing layer is assumed to be known and, in the present study, is assumed to be constant. Initial conditions were specified at the start of the jet corresponding to uniform jet properties for $r \le r_j$ and uniform freestream properties for $r > r_j$.

Results and Discussion

In this section, both one-scale and two-scale turbulence closure models are used in the SCIPVIS code to predict the in-

teraction of an underexpanded supersonic jet ($1 < M_j < 2$) with the surrounding external stream. The one-scale models used in this study are 1) $k\epsilon$2-*cc*, compressibility corrected version of $k\epsilon$2 mode; 2) $k\epsilon$2 model without compressibility correction; and 3) *KW* model of Spalding.[17] The two-scale (2*S*) models used in this study are 1) $k\epsilon$2-2*S*-*cc*, compressibility corrected, two-scale $k\epsilon$2 model; 2) $k\epsilon$2-2*S*, two-scale model without compressibility correction; and 3) $k\epsilon$2-2*S*-*T*1 and $k\epsilon 2 + 2S$-*T*2, two-scale models with dissipation related to time scale.

The predictions are compared to the experimental data of Norum and Seiner[18] that were obtained for jets exhausting into nominally still air. Because of numerical limitations in the SCIPVIS code, calculations could not be made with the external Mach number set exactly to zero. Therefore, all calculations presented are for an external stream at a Mach number of 0.25. Sensitivity studies showed that varying this arbitrary value by as much as ±0.1 produced no significant effect on the predicted jet pressure distributions. Comparisons are presented for static pressure distributions measured along the jet centerline. Additional comparisons of selected off-axis locations are given in Ref. 19. Three test cases were selected for study: 1) underexpanded, cold-air, supersonic jet, $M_j = 2.0$, $P_j = P_a = 1.45$; 2) underexpanded, cold-air supersonic jet, $M_j = 1.4$, $P_j/P_a = 1.36$; and 3) underexpanded, cold-air, sonic jet, $M_j = 1.0$, $P_j = P_a = 1.62$.

Results for these cases have been presented in Ref. 1 for the one-scale models. Those results included calculations made with the *KW* model of Spalding,[17] which also are included here for completeness. Since the details of the initial profiles and other numerical parameters used for those calculations were not available, all cases were recalculated for the present study to ensure that comparisons with the two-scale results would be made for the same initial conditions.

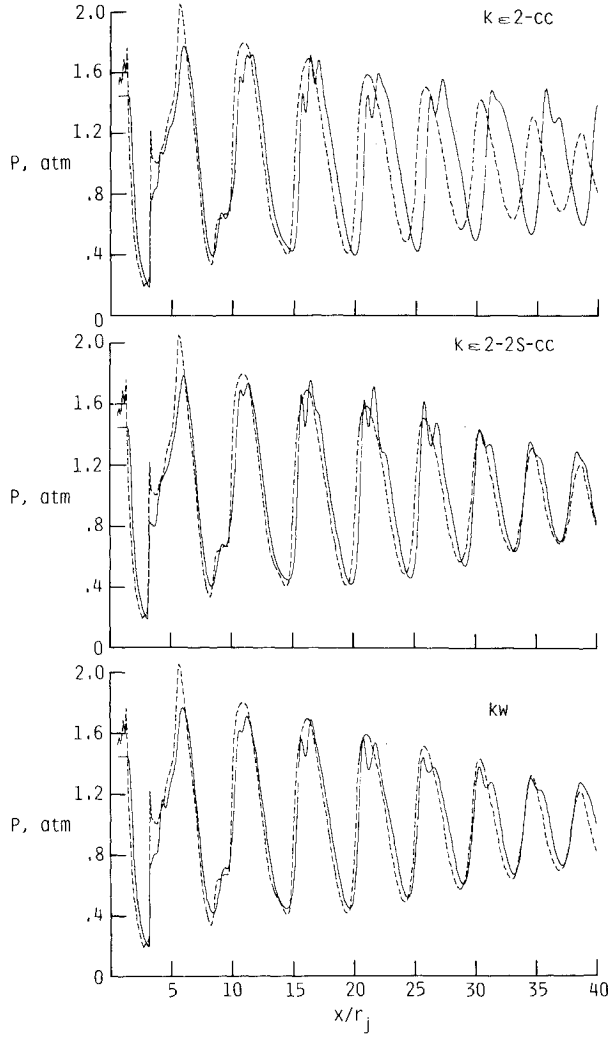

Fig. 3 Comparison of predicted ($k\epsilon$2-*cc*, $k\epsilon$2-2*S*-*cc*, and *kW*) and measured centerline pressure for underexpanded $M_j = 2.0$ jet.

For the present calculations, the initial profiles of k, ϵ, k_P, k_T, ϵ_P, ϵ_T, and W are estimated from the mixing-length model based upon the mean flow profile. The mixing-length model relates μ_t to the local gradient through the relation

$$\mu_t(r) = \rho \ell^2 \frac{\partial U}{\partial r} \tag{11}$$

where ℓ is an initial mixing-length scale estimated from spread rates for incompressible shear layers (see Ref. 20 for details).

Assuming $P/\epsilon = 1$, we obtain

$$k(r) = \frac{\mu_t(r)\,(\partial U/\partial r)}{0.3\rho(r)} \tag{12a}$$

$$\epsilon(r) = 0.09\rho(r)k^2(r)/\mu_t(r) \tag{12b}$$

The two turbulent quantities k and ϵ then may be used to estimate the initial profiles for the two-scale quantities k_P, k_T, ϵ_P, and ϵ_T. A nonequilibrium initial state for the turbulence level was assumed. For convenience in describing the initial two-scale distributions, the following relations are defined:

$$k_P = \frac{a}{a+b}k, \quad k_T = \frac{b}{a+b}k, \quad \epsilon_P = \epsilon, \quad \epsilon_T = \frac{c}{c+d}\epsilon_P \tag{13}$$

where a, b, c, and d are constants having a value of 0.5 in most cases. The absolute values of a, b, c, and d also are used as limiting values of k_P, k_T, ϵ_P, ϵ_T outside the mixing layer of the jet. It should be noted that since the actual values of k_P, k_T, ϵ_P, and ϵ_T are determined from the discretized initial profiles of U, the magnitudes of initial turbulence and dissipation may depend strongly on the profile shape and number of radial grid points. Identical initial data are used for the three different test cases (i.e., with the same integration options, initial profiles, and number of nodes along the radial axis r).

Case 1: $M_j = 2.0$, $P_j/P_a = 1.45$

Figure 3 shows a comparison of the results predicted using the different turbulence models with the measured streamwise pressure variation along the jet centerline. The jet was operated at a pressure ratio of 1.45, corresponding to a fully expanded Mach number of 2.24, and was issued from a convergent-divergent nozzle with a design Mach number of 2.

The measured static pressure distributions illustrate the decaying shock structure that occurs due to the interaction of the shocks with the growing mixing layer. All three turbulence models predict this decay with varying degrees of success. The $k\epsilon$2-*cc* model predicts the pressure variations up through the first five shock cells and significantly underestimates the rest of the shock-cell decay. This indicates that the growth of the mixing layer and turbulent dissipation of the shock strengths are not properly modeled using the $k\epsilon$2-*cc* one-scale model. The same observations have been made by Dash and Wolf[21] for this case.

Both the $k\epsilon$2-2*S*-*cc* (Fig. 3b) and *kW* (Fig. 3c) model predictions show much improvement over the $k\epsilon$2-*cc* predictions. Both the shock-cell spacings and pressure amplitudes agree extremely well. The agreement with experiment for both a single-scale (*kW*) model and a two-scale ($k\epsilon$2-2*S*-*cc*) model indicates that multiscale effects are probably not very important in this Mach 2 case. In fact, all three models predict the overall axial decay in peak shock-cell pressures reasonably well, although there is considerable disagreement in phase in the axial direction for the $k\epsilon$2-*cc* results.

Comparisons of turbulence intensity between $k\epsilon$2-*cc* and *kW* model predictions and experiment have been presented in Ref. 3, and reasonably good agreement was obtained. The present two-scale model gives similar agreement. However, because of the limited amount of data available, no conclusion can be drawn as to which model provides the best prediction of turbulence intensity. It may be stated that for the Mach 2 jet, the observed pressure distribution along the centerline is not extremely sensitive to the details of turbulence in the near-field mixing region.

Case 2: $M_j = 1.4$, $P_j/P_a = 1.36$

Figure 4 shows the comparison of $k\epsilon$2-*cc*, $k\epsilon$2-2*S-cc*, and *KW* predictions with measured centerline pressures for a jet operated at a pressure ratio of 1.36, corresponding to a fully expanded Mach number of 1.62 and a design Mach number of 1.41.

Experimental data are available only for the first two shock cells. All three models give good agreement with these limited results. It is noted that the $k\epsilon$2-2*S-cc* (two-scale) model predicts a more rapid decay in the peak shock-cell pressure downstream of the first six shock cells than either of the one-scale models. However, the lack of experimental data in this region does not allow the accuracy of these predictions to be assessed.

Case 3: $M_j = 1.0$, $P_j/P_a = 1.62$

Experimental data are shown in Fig. 5 for a sonic nozzle operating at $P_j/P_a = 1.62$, corresponding to a fully expanded Mach number of 1.37. The centerline pressure oscillations decay abruptly after the fifth shock cell ($x/r_j > 10$). Acoustic data obtained under similar jet conditions suggest that such phenomena may be caused by acoustic resonance.[4] In such cases, it is postulated that acoustic waves generated by the shock-cell structure feed upstream through the subsonic portion of the mixing layer at such a frequency as to cause the rapid growth of turbulent instabilities, which eventually dominate the plume structure. Previous calculations of such cases using one-scale turbulence models[3] were not able to predict this decay. One of the principal reasons for the present interest in multiscale effects is to determine if the multiscale models can at least qualitatively predict the enhanced mixing in these highly resonant cases. For this reason, the sonic jet case was studied more extensively, and several modifications to the basic two-scale model were applied.

As with most marching codes, SCIPVIS was not able to run with the jet exit Mach number set precisely at 1.0. Therefore, a Mach number of 1.02 is used as an initial value for the calculations discussed in this section.

Basic Model Comparisons

Figure 6 shows the results predicted with the $k\epsilon$2-*cc*, $k\epsilon$2-2*S-cc*, and *kW* turbulence models compared to the measured pressures along the centerline. All three calculations show reasonable agreement up through the first five shock cells, although there is some disagreement in amplitude after the first cell. However, all three calculations greatly underpredict the shock-cell decay after the fifth cell. Comparing the various calculated results, the $k\epsilon$2-2*S-cc* and *kW* models show a faster shock-cell decay than the $k\epsilon$2-*cc* predictions, with the two-scale results showing the most rapid decay of any of the models. It is not clear at this time that these disagreements

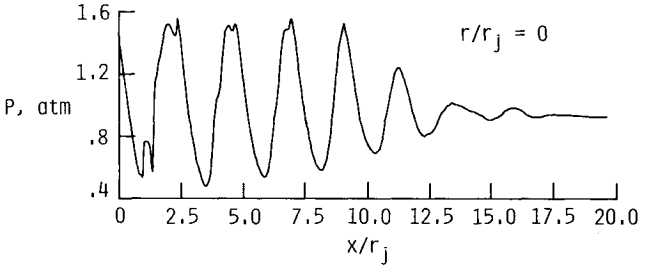

Fig. 5 Measured plume pressures at $r/r_j = 0.0$ for underexpanded sonic jet.

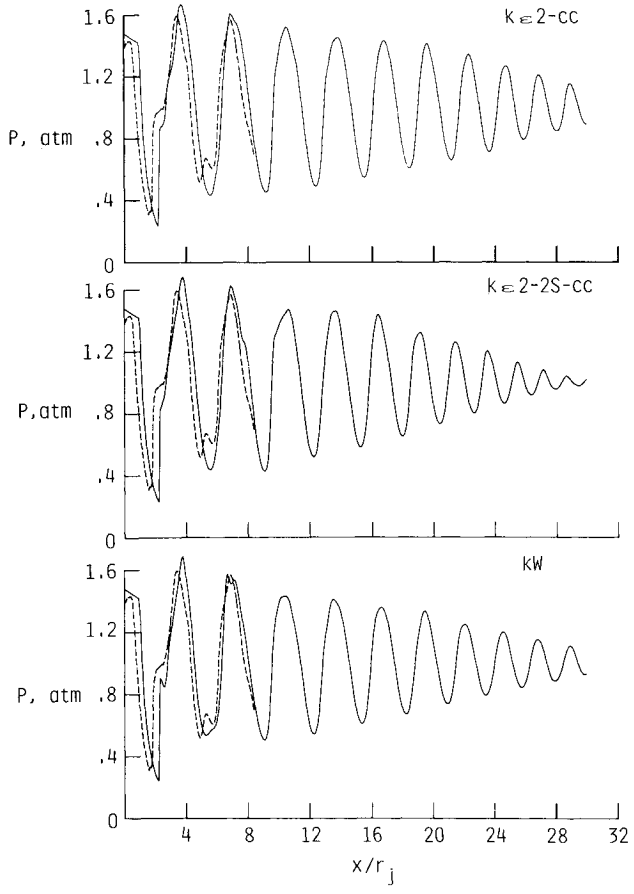

Fig. 4 Comparison of predicted ($k\epsilon$2-*cc*, $k\epsilon$2-2*S-cc*, and *kW*) and measured centerline pressure for underexpanded $M_j = 1.41$ jet.

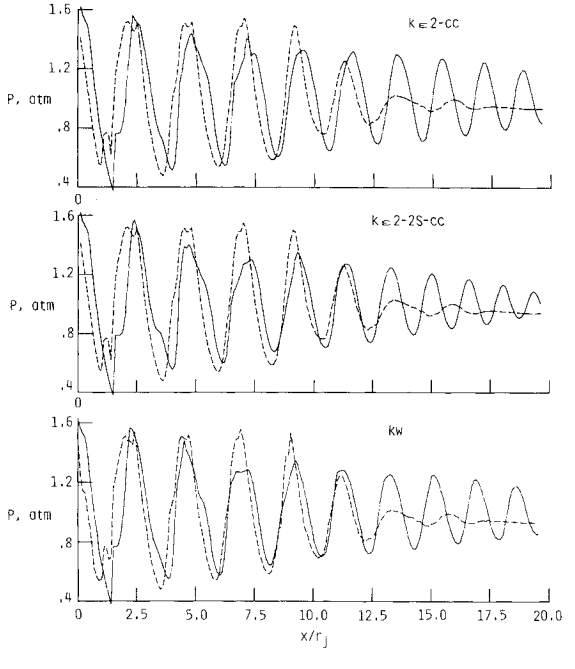

Fig. 6 Comparison of predicted $k\epsilon$2-*cc*, $k\epsilon$2-2*S-cc*, and *kW* and measured centerline pressure for underexpanded sonic jet.

with experiment are related only to turbulence modeling but may also be due to the limitations of the basic computational model. That is, if acoustic resonance is occurring through upstream influence in the subsonic portion of the mixing layer, then elliptic effects (which are absent in the present calculations) must be considered. It is clear from these comparisons that none of the three turbulence models provides an accurate representation of the flowfield of the sonic jet.

The experimental results shown in Fig. 5 show that after the initial jet mixing region, the average static pressure falls below atmospheric. Near the end of the transition zone, there is a general recovery of the centerline static pressure.[3] This phenomena shows that the pressure in the subsonic region of the shear layer is varying with x/r_j. The SCIPVIS code solves the Parabolized Navier-Stokes (PNS) equations and assumes the pressure in the elliptic (subsonic) zone is constant and equal to the upper boundary pressure (atmospheric). Thus, the calculated static pressure will always approach the atmospheric value asymptotically.

Effect of Compressibility

Based on the assumption that incompressible turbulence models may be used to calculate compressible mixing layers for turbulent Mach numbers close to and less than 1, it is worthwhile to drop the compressibility correction function and repeat the calculations using the $k\epsilon 2$ and $k\epsilon$2-2*S* models. Figure 7 shows the results for these two models (without compressibility correction) compared to experiment. The $k\epsilon 2$ model still underestimates the shock-cell decay and, therefore, presumably the growth of the mixing layer. However, dropping the compressibility correction has a significant effect on the two-scale model predictions. The $k\epsilon$2-2*S* result shows a rapid decay in the pressure beyond the jet potential core and shows much more favorable agreement with experiment. Even though the axial location of all shock cells do not match the measured data, it is clear that the two-scale turbulence model $k\epsilon$2-2*S* provides a better representation of the overall shock-cell decay (and, therefore, the turbulent mixing) than either of the one-scale models.

Figure 8 shows the predicted centerline total turbulent kinetic energy for the two models. The $k\epsilon$2-2*S* calculation shows a rapid increase in total turbulent kinetic energy downstream of $x/r_j = 15$, which corresponds closely to the observed rapid decay in centerline static pressure. As a result of the slower mixing predicted with the $k\epsilon 2$ model, the mixing reaches the axis much further downstream, and the calculated turbulent kinetic energy shows a slow increase over the region shown.

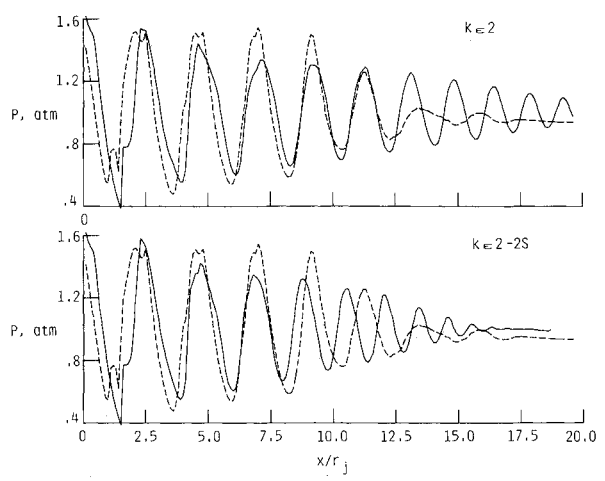

Fig. 7 Comparison of predicted ($k\epsilon 2$ and kϵ2-2*S*) and measured centerline pressure for underexpanded sonic jet.

Modified Time-Scale Model

Hajalic[5] and Chen[6,7] suggest that some of the "constants" in the turbulent transport equations for k_p, ϵ_p, k_T, and ϵ_T may somehow vary with the production and transfer mechanisms. Based on the experimental data for the Mach 1 jet, it is obvious that some mechanism is needed to explain the rapid decay in centerline pressure for $x/r_j > 10$. Abdol-Hamid and Wilmoth[11] studied the effect of initial and limiting values of the transfer kinetic energy and dissipation on the turbulent mixing of the plume. They concluded that the turbulent mixing rate is related to the time-sale ratio T between the two spectral regions and found that the predicted time ratio drops to values less than one for the sonic jet for $x/r_j > 10$. Therefore, the two-scale model was modified by replacing the term $\rho\epsilon_T$ with $F(T)\rho\epsilon_T$ in the k_T transport equation. Two different arbitary functions for $F(T)$ were proposed in Ref. 11:

$k\epsilon$2-2*S*-*T*1:

$$F(T) = 1 \qquad T > 1$$
$$= T \qquad T < 1$$

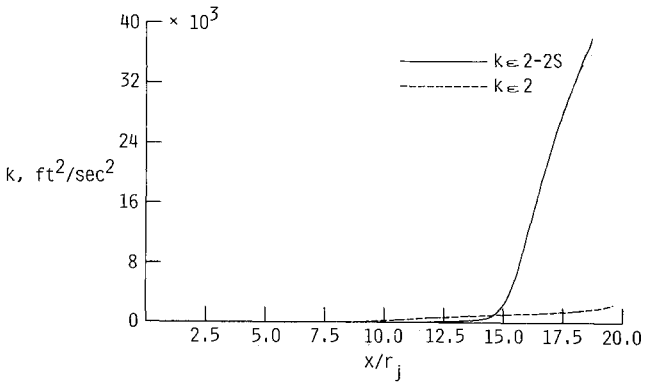

Fig. 8 Comparison of total turbulent kinetic energy calculated using $k\epsilon 2$ and $k\epsilon$2-2*S* for underexpanded sonic jet.

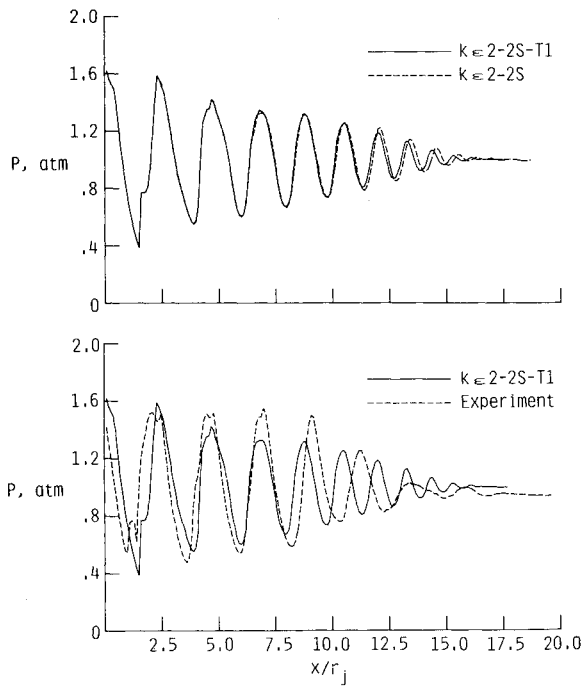

Fig. 9 Prediction of centerline pressures using modified time-scale model, $k\epsilon$2-3*S*-*T*1, for underexpanded sonic jet.

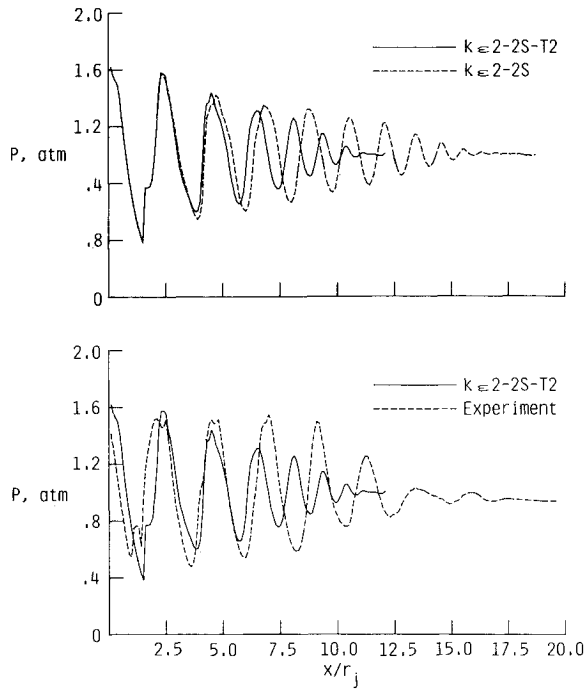

Fig. 10 Prediction of centerline pressures using modified time-scale model, $k\epsilon$2-2*S*-*T*2, for underexpanded sonic jet.

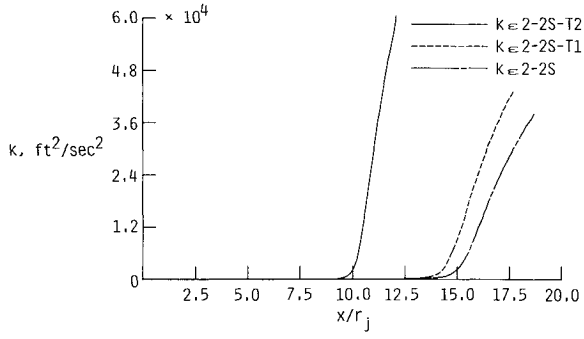

Fig. 11 Comparison of calculated total kinetic energy for sonic jet using $k\epsilon$2-2*S*, $k\epsilon$2-2*S*-*T*1, and $k\epsilon$2-2*S*-*T*2.

$k\epsilon$2-2*S*-*T*2:

$$F(T) \begin{matrix} = 1/T & T>1 \\ = T & T<1 \end{matrix}$$

Each of these functions is constructed to decrease the effective transfer dissipation for $T<1$, thereby increasing the transfer kinetic energy and presumably the turbulent mixing in the downsteam region of the jet.

Figure 9 shows a comparison between the centerline pressure predictions using $k\epsilon$2-2*S*-*T*1 and $k\epsilon$2-2*S* and between $k\epsilon$2-2*S*-*T*1 and experiment. In general, $k\epsilon$2-2*S*-*T*1 shows a slight improvement in the agreement with experiment over $kt2+2S$. In the near field, both models have the same pressure variations, whereas in the far field, there is a slight decrease in shock-cell spacing. Figure 10 shows a similar comparison of the $k\epsilon$2-2*S*-*T*2 results with $k\epsilon$2-2*S* and experiment. The $k\epsilon$2-2*S* model shows a very rapid decay in the centerline static pressure as compared to $k\epsilon$2-2*S* and shows a faster decay than even the experimental results. Figure 11 shows the comparison between total kinetic energy produced by $k\epsilon$2-2*S*, $k\epsilon$2-2*S*-*T*1, and $k\epsilon$2-2*S*-*T*2 turbulence models. The $k\epsilon$2-2*S*-*T*2 calculation shows a rapid increase in turbulent kinetic energy near $x/r_j = 10$, which corresponds closely to the observed rapid decay in centerline static pressure, whereas the other two models predict the rise to occur further downstream. (The rise in centerline turbulent kinetic energy occurs as the mixing reaches the axis of the jet.)

As a final note, it may be observed that the $k\epsilon$2-2*S*-*T*1 and $k\epsilon$2-2*S*-*T*2 results appear to approximately bound the experimental centerline pressure distribution at least insofar as the overall pressure decay is concerned. However, none of the model predictions gives good results for both shock-cell decay and spacing. Since a major deficiency of the present computational model is the neglect of upstream influence of pressure disturbances on the turbulent mixing and shock interaction, it would be interesting to study these effects using a computational model that could fully account for these elliptic effects. For proper modeling of jet plumes where such resonance behavior occurs, such a computational model would appear to be essential.

Concluding Remarks

A modified version of the multiscale turbulence model of Hanjalic has been applied to the problem of underexpanded supersonic jets exhausting into still air. In particular, the problem of shock-cell decay resulting from shock-mixing layer interactions has been addressed for both mildly interacting and strongly resonant jet conditions. The two-scale model takes into account the nonequilibrium spectral energy transfer mechanism. The key to the two-scale model is the recognition that the dominant production and dissipation mechanisms may occur in different spectral regions. Such a model allows for the possibility that production occurs in the large eddies of the flow, whereas dissipation involves maintly the smaller scales. Steady-state, parabolized versions of the Hanjalic model with ($k\epsilon$2-2*S*-*cc*) and without ($k\epsilon$2-2*S*) compressibility corrections were incorporated into the SCIPVIS code to provide a computational framework for testing the validity of the two-scale model.

In general, the two-scale model provides improvement over the one-scale models in the prediction of the plume structure for underexpanded supersonic ($M_j = 2$ and 1.4) and sonic ($M_j = 1$) jets. For the supersonic jet cases studied, excellent agreement was obtained with measured shock-cell pressure decay along the jet centerline. For the sonic jet case, the agreement with experiment was not as good, but the two-scale model still showed significant improvement over one-scale turbulence model results. Although exact agreement was not obtained in the sonic jet, it has been shown that by relating certain coefficients in the turbulent transport equations to the relative time scale for transfer of energy between turbulent scales, the two-scale model can provide predictions that approximately bound the experimental data.

Further understanding is obviously needed on the details of the production and dissipation of large-scale turbulent structures in jets before an adequate model can be constructed for predicting the turbulent mixing in highly resonant jet plumes. Better modeling of the interaction between acoustic disturbances and turbulent instability modes is especially needed. Improvements in the computational models perhaps could be made by incorporating the present two-scale model into a computational method that can account for elliptic effects (e.g., global-relaxation parabolized Navier-Stokes or time-dependent Navier-Stokes methods). However, the multiscale turbulence model at least may provide an additional degree of empiricism that can be used for practical estimates of plume mixing over a wider range of jet conditions than can be made with existing single-scale models.

References

[1]Dash, S. M. and Wolf, D. E.,"Fully-Coupled Analysis of Jet Mixing Problems, Part I: Shock-Capturing Model SCIPVIS," NASA CR-3761, Jan. 1984.

[2]Tam, C. K. W., Jackson, J. A., and Seiner, J. M. "A Multiple-Scales Model of the Shock-Cell Structure of Imperfectly Expanded Supersonic Jets," *Journal of Fluid Mechanics*, Vol. 153, April 1985, pp. 123–149.

[3]Seiner, J. M., Dash, S. M., and Wolf, D. E.," Shock Noise Features Using the SCIPVIS Code," AIAA Paper 83-0705, April 1983.

[4]Seiner, J M., "Advances in High-Speed Jet Acoustics," AIAA Paper 84-2275, Oct. 1984.

[5]Hanjalic, K., Launder, B. E., and Schiestel, R., "Multiple-Time-Scale Concepts in Turbulent Transport Modeling," *Turbulent Shear Flow,* Vol. 2, edited by L. J. S. Bradbury, F. Durst, B. E. Launder, F. W. Schmidt, and J. H. Whitelaw, Springer-Verlag, Berlin, 1980, pp. 36–49.

[6]Chen, C. P., "Multiple-Scale Turbulence Closure Modeling of Confined Recirculating Flows," NASA CR-178536, Aug. 1985.

[7]Chen, C. P., "Confined Swirling Jet Predictions Using a Multiple-Scale Turbulence Model," NASA CR-178484, Aug. 1985.

[8]Hanjalic, K. and Launder, B. E.,"A Reynolds Stress Model of Turbulence and Its Application to Thin Shear Flows," *Journal of Fluid Mechanics*, Vol. 52, April 1972, p. 609.

[9]Launder, B. E., Reece, G. J., and Rodi, W., "Progress in the Development of a Reynolds-Stress Turbulence Closure," *Journal of Fluid Mechanics,* Vol. 68, April 1975, pp. 537–566.

[10]Wilcox, D.C., "Multiscale Model for Turbulent Flows," AIAA Paper 86-0029, Jan. 1986.

[11]Abdol-Hamid, K. S. and Wilmoth, R. G., "Multiscale Turbulence Effects in Supersonic Jets Exhausting into Still Air," NASA TP-2707, 1987.

[12]Tennekes, H. and Lumley, J. L., *A First Course in Turbulence,* MIT Press, Cambridge, MA, 1972.

[13]Morkovin, M. V., "Effects of Compressibility on Turbulent Flows," *The Mechanics of Turbulence,* edited by A. Favre, Gordon and Breach, New York, 1964, p. 367.

[14]Fabris, G., Harsha, P. T., and Edelman, R. B., "Multiple-Scale Turbulence Modeling of Boundary Layer Flows for Scramjet Applications," NASA CR-3433, May 1981.

[15]Rodi, W., *Turbulence Models and Their Application in Hydraulics,* IAHR-Section on Fundamentals of Division II: Experimental and Mathematical Fluid Mechanics, 1984.

[16]Dash, S. M., Weilerstein, G., and Vaglio-Laurin, R.," Compressibility Effects in Free Turbulent Shear Flows," Air Force Office of Scientific Research, AFOSR-TR-75-1436, 1975; (available from Defense Technical Information Center, Cameron Station, Alexandria, VA, AD A016 535).

[17]Spalding, D. B., "Concentration Fuctuations in Round Turbulent Free Jet," *Chemical Engineering Science,* Vol. 26, 1971, p. 95.

[18]Norum, T. D. and Seiner, J. M., "Measurements of Mean Static Pressure and Far Field Acoustics of Shock-Containing Supersonic Jets," NASA TM-84521, Sept. 1984.

[19]Abdol-Hamid, K. S. and Wilmoth, R. G., "Multiscale Turbulence Effects in Underexpanded Supersonic Jets," AIAA Paper 87-1377, June 1987.

[20]Dash, S. M., Pergament, H. S., and Thorpe, R. D., "Computational Models for the Viscous/Invscid Analysis of Jet Aircraft Exhaust Plumes," NASA CR-3289, May 1980.

[21]Dash, S. M. and Wolf, D. E., "Interactive Phenomena in Supersonic Jet Mixing Problems," AIAA Paper 83-0288, Jan. 1983.